

Long-range and very long-range charge transport in DNA

M. Bixon, Joshua Jortner*

School of Chemistry, Tel Aviv University, Ramat Aviv, 69978 Tel Aviv, Israel

Received 11 June 2001

Abstract

We present a kinetic–quantum model for the mechanisms of hole transport in DNA duplexes, which involves a sequence of hole hopping processes between adjacent guanines (G) and/or hole hopping/trapping via GG or GGG, all of which are separated by thymine (T)–adenine (A) bridges. Individual hole hopping processes between G sites fall into two distinct parallel mechanisms, i.e., unistep superexchange mediated hopping via ‘short’ $(T-A)_n$ bridges and thermally induced hopping (TIH) via ‘long’ $(T-A)_n$ ($n > 3-4$) bridges. The bridge specificity for TIH via $(A)_n$ chains pertains to the energetics, with the G^+A energy gap $\Delta = 0.20 \pm 0.05$ eV being sufficiently low to warrant endothermic hole excitation from G^+ to $(A)_n$, and to the electronic couplings, with the nearest-neighbor A–A couplings being unique in the sense that the intrastrand and interstrand couplings are close and large ($V(A-A) \simeq 0.30-0.060$ eV). Accordingly, both effective intrastrand and interstrand (zigzagging) hole transport via $(A)_n$ chains will prevail, being nearly invariant with respect to the nucleobases ordering within the $(T-A)_n$ duplex. We treated the ‘transition’ between the superexchange and the TIH mechanism in $5'-G^+(T-A)_nG-3'$ duplexes to predict that the crossover occurs at $n_x \simeq 3-4$, with n_x exhibiting a moderate bridge specificity and energy gap dependence. n_x is in accord with the experimental data of Giese et al. [Nature 412, 318, 2001]. We assert that the kinetic–quantum mechanical model for the chemical yields and elementary rates cannot be reconciled with the experimental TIH data, with respect to the very weak bridge size dependence of the relative chemical yields and the ratios of the rates. Configurational relaxation accompanying endothermic hole injection from G^+ to $(A)_n$ may result in the gating (switching-off) of the backrecombination, providing a reasonable description of TIH dynamics and very long-range hole transport in long $(A)_n$ chains. © 2002 Published by Elsevier Science B.V.

1. Introduction

Molecular wires constitute nanostructures whose spatial configuration, energetics, nuclear and electron dynamics promote long-range charge transport [1–10]. DNA based molecular electronic

devices are expected to utilize the unique features of recognition, assembly and specific binding properties of the nucleobases, with the DNA duplexes serving as building blocks or/and templates for the assembly and function of electronically active nanoelements [11–18]. The elucidation of the role of DNA as a ‘molecular wire’ requires the establishment of the dynamics and mechanism of charge transport. Two limiting classes of nanostructured ‘molecular wires’ should be

* Corresponding author. Fax: +972-3-6415054.

E-mail address: jortner@chmsg1.tau.ac.il (J. Jortner).

distinguished on the basis of their charge transport mechanism, i.e., ballistic band motion and charge hopping between localized states [9,19]. Neat, undoped DNA falls into the second category, constituting a ‘vibronic molecular wire’ where hopping transport prevails [20–27]. The charge hopping mechanism in DNA is described in terms of the quantum mechanical non-adiabatic electron transfer theory [19], with the ingredients of electronic (direct exchange or superexchange) coupling, and nuclear coupling with low-frequency intermolecular and medium modes together with high-frequency intramolecular modes. This approach can be considered as an extension of the Holstein small polaron model [28] in the non-adiabatic limit, extended to account for the important effects of intramolecular nuclear distortion (reorganization) of the nucleobases. This model for hopping transport in vibronic molecular wires may be referred to as the ‘molecular polaron’.

The majority of the experimental information on charge transport in DNA pertains to the positive charge (hole) migration, i.e., the propagation of the radical cation along the duplex [29–40]. Energetic data and computational results [23,41–44] show that G nucleobases act as ‘resting’, lowest energy states for holes in DNA duplexes, while GG and GGG doublets/triplets act as shallow hole traps in DNA, in accord with the experimental data [29–37]. The interrogation of individual elementary steps of charge injection, trapping, hopping, and recombination, and their lifetimes in (intercolated, substituted or capped) DNA was accomplished by utilizing the arsenal of the methods of nanosecond to femtosecond time-resolved spectroscopy [33–35,45,46]. Concurrently, information on hole trapping was inferred from terminal/proximal $(GGG)^+/G^+$ relative chemical yield data induced by hole shift in $G^+(T-A)_nGGG$ ($n = 1-4$; distance scale 10–40 Å) duplexes [36–38,43]. Experimental evidence for long-range hole transport over distance scales of 40–200 Å [29–32,36–40,47,48] emerged from terminal/proximal guanine relative chemical yield data, which are induced by photochemical hole injection from an electronically excited donor (i.e., from Rh^{+3} complexes [31,32], from anthraquinone [29,39,40]), or from chemical hole shift (from a sugar cation [30,36–38,47,48]).

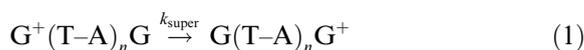
The concept of (donor–bridge) energetic control [20] in DNA, advanced in 1998, provided a unified description of the distinction between off-resonance ($\Delta E > 0$), superexchange induced, short-range unistep charge transfer, and resonance-coupled ($\Delta E < 0$), long-range multistep charge hopping transport. However, the concept of energetic control is strictly valid only at sufficiently low temperatures and for hole transfer between guanine (G) nucleobases separated by sufficiently short $(T-A)_n$ ($n \leq 4$) bridges. Barton and co-workers [32], Giese et al. [47,48] and Bixon and Jortner [22,23,49] proposed that for off-resonance donor–bridge coupling in DNA ($\Delta E > 0$), thermally activated charge injection from G^+ , $(GG)^+$ or $(GGG)^+$ into some nucleobases of the bridge (which are characterized by a higher oxidation potential) followed by multistep hopping among the bridge constituents, can occur at finite temperatures. Most important, it was proposed [32,47–49] that thermally induced hole injection from G^+ to A followed by hopping between A nucleobases will occur. The thermally induced hopping (TIH) process occurs in parallel with the unistep superexchange tunneling. Barton et al. [30] and Giese et al. [47,48] provided strong experimental evidence for TIH through long chain adenine nucleobases ($n = 4-16$ [47,48] and $n = 4-10$ [30]) in DNA. The features of TIH are general, being applicable not only for DNA but also for charge migration in large chemical scale systems, e.g., donor–acceptor pairs bound by polymers, such as oligoproline donor–acceptor complexes [41,50], as well as for the (sequential-superexchange) primary charge separation in biological systems [51,52], and in chemically and mutagenically modified photosynthetic reaction centers [53].

The compound mechanism of long-range hole transport in a duplex $dG_1(T-A)_nG_2 \cdots G_Nt$ containing N guanine nucleobases separated by $(T-A)_n$ bridges between a donor (d) and acceptor (trap) t, e.g., G, GG or GGG, involves several steps: (i) hole injection from d to the proximal G_1 ; (ii) a sequence of hole hopping processes between adjacent guanines, i.e., G_j and $G_{j\pm 1}$ within the bridge; and (iii) termination by hole trapping/de-trapping between G_N and t. The individual hole

hopping processes (ii) between G_j and $G_{j\pm 1}$ fall into two categories:

1.1. Hopping mechanism A

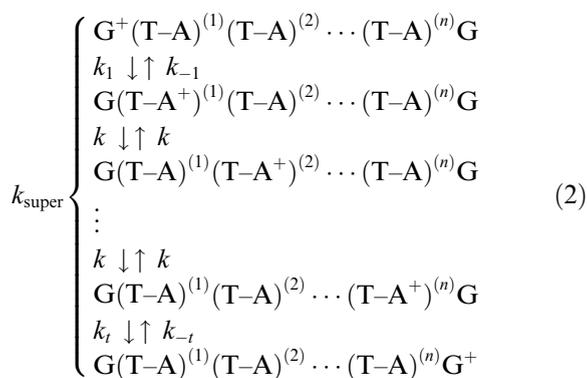
Unistep superexchange mediated hopping [20–27,31–38,47–49]. For moderately short $(T-A)_n$ bridges ($n \leq 4$) each hopping step is induced by superexchange, off-resonance electronic coupling between G_j and $G_{j\pm 1}$ via the $(T-A)_n$ subbridges. The hole states of the $(T-A)_n$ subbridge are virtual and do not constitute a real chemical intermediate. The kinetic scheme for the individual unistep superexchange hopping rate is



This physical picture of unistep hole superexchange between guanines separated by ‘short’ $(T-A)_n$ ($n \leq 4$) subbridges was proposed and analysed in detail [20–27,49] to account for the experimental yield data of Giese et al. [30,36–38], Saito et al. [54,55] and Barton and co-workers [56]. Regarding the compound hole transport mechanism, the unification of $G \cdots G$ superexchange mediation and $G \cdots G$ hopping accounts for multistep long-range hole transport, with each hopping step involving superexchange via ‘short’ ($n \leq 4$) subbridges.

1.2. Hopping mechanism B

Thermally induced hopping (TIH) [22,23,25,30,47–49]. This mechanism prevails in ‘long’ $(T-A)_n$ ($n \geq 4$) bridges, which separate between G_j and $G_{j\pm 1}$ nucleobases. Each bridge with its proximal/terminal guanines will be denoted by $G_j(T-A)^{(1)}(T-A)^{(2)} \cdots (T-A)^{(n)}G_{j\pm 1}$. Hole transport via TIH within the subbridge will occur via thermally induced donor–bridge hole excitation from G^+ to A in $(T-A)^{(1)+}$ (rate k_1), followed by hole hopping between nearest-neighbor A nucleobases (see Section 2) within the bridge (hopping rates k) and being terminated by hole trapping (rate k_t). The kinetic scheme also has to include hole deexcitation (rate k_{-1}) and hole detrapping (rate k_{-t}) from/to the adenines bridge. The kinetic scheme for the hole TIH between G_j and $G_{j\pm 1}$ is given by Eq. (2),



Most important, the endothermically accessible (via $G^+A \rightarrow GA^+$ thermal excitation and $A^+A \rightarrow AA^+$ hopping) A^+ cations constitute genuine chemical intermediates, which are amenable to interrogation by magnetic or optical spectroscopy. This compound hole transport mechanism involves $G \cdots G$ charge transport via a set of charge hopping steps through the A nucleobases, allowing for very long-range hole transport via ‘long’ $(T-A)_n$ ($n > 3$) subbridges [47–49]. The TIH occurs in parallel with the unistep superexchange tunneling (mechanism (A)) [22,47–49].

The unistep superexchange mediated hopping (mechanism (A)) was explored in considerable detail [20–27,49] incorporating the effects of subbridge length, of the sequence specificity of the $(G-A)_n$ subbridge, of backtrapping and of side reactions of G^+ with water. On the other hand, the theoretical [47–49] information on TIH in DNA (mechanism (B)) is still limited, and will be explored in the present paper.

2. Thermally induced hopping via adenine chains and the crossing between superexchange and TIH in DNA

2.1. The TIH mechanism

We shall now address the mechanistic issues of hole TIH via $(A)_n$ chains in $G^+(T-A)_n G$ duplexes, considering the characteristics of bridge specificity and of the ‘critical’ $(T-A)_n$ bridge size for the onset of the TIH mechanism. In the following treatment, as well as in the kinetic–quantum mechanical

analysis presented in Section 3, we consider a rigid DNA structure, which is determined by the (average) nuclear equilibrium configuration. The nuclear configurational fluctuations of the DNA duplex, of the sugars and phosphates, of water and of alkali cations, may affect the energetics and the electronic couplings. These effects of configurational fluctuations, which are determined by the relative time scales for the electronic processes and of the fluctuations, will not be considered herein. We shall also neglect any possible effects of configurational relaxation accompanying charge injection from G^+ to the $(A)_n$ chain or charge trapping from the $(A)_n^+$ chain by G.

In the context of bridge specificity, we have to consider both the energetics and the electronic couplings. Consider first the energetics of TIH. On the basis of the hierarchy of the oxidation potentials of the nucleobases ($G < A < C, T$) [40–44], the A nucleobases (with a moderately low energy gap of $\Delta = 0.20 \pm 0.05$ eV between G^+A and GA^+ , as determined [49] from a kinetic analysis of endothermic hole hopping [57] in DNA) constitute hole carriers in TIH between the guanines (Fig. 1). This conclusion is in accord with the TIH proposal and experiments of Giese et al. [47,48] and our theoretical modeling [49] of the energetics and kinetics of the TIH. The kinetic analysis of a simple model for the TIH process, Eq. (2), which neglects side reactions of G^+ with water (Section 3), implies (see Eq. (A.16)) that the rate k_{TIH} of hole transfer from the proximal G is given by

$$k_{\text{TIH}} = k \exp(-\Delta/k_{\text{B}}T) / [(k/k_{-1}) + (k/k_t) + (n-1)], \quad (3)$$

where $\Delta(>0)$ is the energy gap between $G^+(T-A)^{(1)}$ and $G(T-A^+)^{(1)}$, while the elementary hopping (k), trapping (k_t) and deexcitation (k_{-1}) rates are defined in Eq. (2). Eq. (3) holds for an effective sink, i.e., $k_t/k_{-1} \gg 1$. When effective hole recombination rates are fast, i.e., $n > k/k_t$, k/k_{-1} , one gets

$$k_{\text{TIH}} = k \exp(-\Delta/k_{\text{B}}T) / (n-1). \quad (3a)$$

The algebraic dependence $k_{\text{TIH}} \propto (n-1)^{-1}$ corresponds to the rate of hole transfer from the proximal G. For the rate of the appearance of the hole at the terminal G, we get (Eq. (A.24))

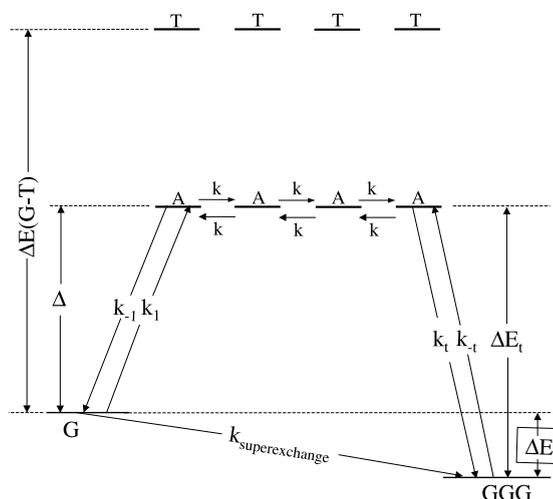


Fig. 1. A kinetic-energetic scheme for the parallel superexchange-TIH mechanism of hole transport in $G^+(T-A)_n$ GGG duplexes. Horizontal lines depict energy levels of the hole states (in the tight binding approximation). The initial/final levels correspond to G/GGG , the adenine A levels are accessible by TIH (for large n) and can also act as superexchange mediators (for small n). The thymine T levels act as superexchange mediators. The energy gaps, Δ (for G^+A), ΔE (for $G^+ \dots (GGG)$), ΔE_t (for $A^+(GGG)$) and $\Delta E(G-T)$ (for G^+T), are marked on the figure. The arrows represent individual rates for endothermic charge injection (k_1), recombination (k_{-1}), hopping (k), and trapping/detrapping (k_t , k_{-t}). k_{super} denotes the unistep superexchange rate.

$k_{\text{TIH}} \propto (n/2)^{-2}$, as appropriate for a diffusion process [20,49]. The hopping rate k between adjacent adenines (which is taken to be equal for both intrastrand and interstrand nearest-neighbor A nucleobases, as discussed above) is given by [19,20]

$$k = \frac{2\pi}{\hbar} |V(A-A)|^2 F(0), \quad (4)$$

where $F(0)$ is the nuclear Franck–Condon factor and $V(A-A)$ is the nearest-neighbor electronic coupling between A nucleobases.

The nuclear Franck–Condon factor, which incorporates both medium and intramolecular vibrational modes, is given by [19,20]

$$F(\delta E) = (4\pi\lambda k_{\text{B}}T)^{-1/2} \exp(-S) \sum_{n=0}^{\infty} \frac{S^n}{n!} \times \exp[-(\delta E + \lambda + n\hbar\omega)^2 / 4\lambda k_{\text{B}}T], \quad (5)$$

where δE is the (free) energy gap (defined as $\delta E > 0$ for endoergic processes), with $\delta E = 0$ for the symmetric charge transfer process in Eq. (4). λ is the medium reorganization energy involving the contribution of the low-frequency medium modes, while the high-frequency intramolecular vibrational modes are characterized by the (mean) vibrational frequency $\hbar\omega$ and coupling S . Eqs. (4) and (5) for the hopping rate are derived on the basis of the electron transfer theory [19]. A first guess for the relevant nuclear parameters is taken from the analysis of Lewis et al. [33–35] of their experimental data for the (free) energy dependence of the hole injection dynamics to DNA

$$\lambda = 0.25 \text{ eV}; \quad \hbar\omega = 0.18 \text{ eV}; \quad S = 5. \quad (6)$$

Next, we consider the electronic couplings $V(\text{A}-\text{A})$ in Eq. (4) between nearest-neighbor A nucleobases. Quantum mechanical calculations of the electronic coupling matrix elements [58,59] reveal (see Fig. 2) that the A–A couplings are unique in the sense that the intrastrand and interstrand couplings are close [58,59] and large, i.e., $V(\text{A}-$

ELECTRONIC COUPLING BETWEEN
NUCLEOBASES (MATRIX ELEMENTS IN eV)

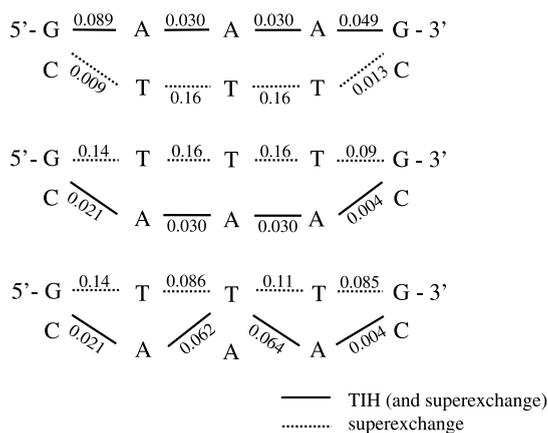


Fig. 2. Electronic coupling matrix elements (from references [58,59]) in eV units, between nearest-neighbor nucleobases in DNA duplexes. Both intrastrand and interstrand electronic couplings are presented. Note that the A–A intrastrand and interstrand electronic couplings are close and large. For other pairs of nucleobases the intrastrand couplings are considerably larger than the interstrand couplings. TIH proceeds via the A nucleobases connected by solid lines. Some routes for superexchange are also marked.

$\text{A}) = 0.030\text{--}0.060$ eV. This pattern of the electronic couplings for A–A is qualitatively different for other nucleobases where the interstrand pair coupling is considerably lower than the intrastrand coupling [58,59]. We infer that effective zigzagging [20], i.e., hole transport between nearest-neighbor intrastrand and interstrand A nucleobases will prevail. In particular, hole transport switching between A nucleobases in the two strands in long $(\text{T}-\text{A})_n$ duplexes may occur. The overall TIH via the $(\text{A})_n$ chain is nearly invariant with respect to the nucleobase ordering within the $(\text{T}-\text{A})_n$ duplex. As every Watson–Crick pair contains either a G or an A nucleobase, a marked erosion of sequence specificity for hole transport via TIH in large $(\text{A})_n$ chains is expected. To conclude this discussion of the TIH rates, Eqs. (3)–(6) and Fig. 2, we note that k_{TIH} manifests a weak, algebraic $(\text{A})_n$ chain length (n) dependence.

2.2. The superexchange mechanism

We now consider the unistep superexchange mechanism, which operates in parallel to the TIH, Eq. (2). The superexchange rate is [19,20]

$$k_{\text{super}} = \frac{2\pi}{\hbar} |V_{\text{super}}|^2 F(\Delta E), \quad (7)$$

where $F(\Delta E)$, Eq. (5), is the nuclear Franck–Condon factor for superexchange (characterized by an energy gap ΔE , with $\Delta E = 0$ for symmetric $\text{G}^+ \cdots \text{G}$ hole shift and $\Delta E = -0.096$ eV for hole trapping in $\text{G}^+(\text{T})_n$ GGG [23]). V_{super} is the superexchange electronic coupling matrix element. Unistep $\text{G} \cdots \text{G}$ superexchange occurs via parallel coupling routes involving both intrastrand and interstrand contributions, with the intrastrand contribution usually being dominant (Fig. 2). The $\text{G} \cdots \text{G}$ superexchange electronic coupling is

$$V_{\text{super}} = \sum_{\text{routes}} \frac{V(\text{G}-\text{X}_{(1)})V(\text{X}_{(n)}-\text{G})}{\Delta(\text{G}-\text{X}_{(1)})} \times \prod_{j=1}^{n-1} \frac{V(\text{X}_{(j)}-\text{X}_{(j+1)})}{\Delta(\text{G}-\text{X}_{(j)})}, \quad (8)$$

where $V(\text{G}-\text{X}_{(1)})$, $V(\text{X}_{(j)}-\text{X}_{(j+1)})$ and $V(\text{X}_{(n)}-\text{G})$ are the nearest-neighbor matrix elements in the duplex $\text{G}^+\text{X}_{(1)}\text{X}_{(2)}\text{X}_{(3)} \cdots \text{X}_{(n)}\text{G}$, which were calculated by

Voityuk et al. [58,59] (Fig. 2). The sum in Eq. (8) is taken over all the coupling routes (Fig. 2), where often a single contribution dominates [59]. The energy gaps $\Delta(\text{G}-\text{X}_{(1)})$ with $\text{X}_{(1)} = \text{T}$ or A are taken as [20] $\Delta(\text{G}-\text{T}) = 0.6$ eV and $\Delta(\text{G}-\text{A}) \equiv \Delta = 0.20$ eV [49]. As expected, $|V_{\text{super}}|^2$ and k_{super} exhibit an exponential distance (n) dependence (Fig. 3).

The unistep superexchange process in the duplex $\text{G}^+(\text{T})_n \text{GGG}$ studied by Giese et al. [36–38,48] is characterized by the rate $k_{\text{super}}(n)$. The dominant contribution to V_{super} , Eq. (8), originates from the interstrand coupling, whereupon

$$V_{\text{super}}(n) = \frac{V(\text{G}-\text{T})V(\text{T}-\text{G})}{\Delta(\text{G}-\text{T})} \left[\frac{V(\text{T}-\text{T})}{\Delta(\text{G}-\text{T})} \right]^{n-1}. \quad (8a)$$

The bridge size dependence of the superexchange rate, Eq. (8a), is

$$k_{\text{super}}(n) = k_{\text{super}}(1)r^{n-1}, \quad (9)$$

where the reduction factor of the rate, upon the addition of a single T nucleobase, is

$$r = \left| \frac{V(\text{T}-\text{T})}{\Delta(\text{G}-\text{T})} \right|^2 = \exp(-\beta R_0) \quad (10)$$

$r = 0.07$ – 0.10 , being alternatively expressed by an exponential with $\beta = 0.79$ – 0.68 \AA^{-1} and $R_0 = 3.38 \text{ \AA}$ is the interbase intrastrand (T–T) spacing. $k_{\text{super}}(1)$ is the superexchange rate for $n = 1$.

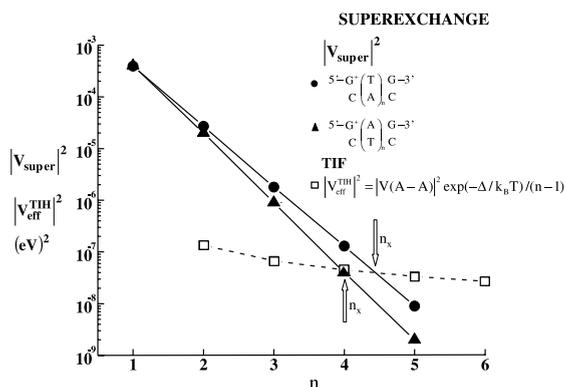


Fig. 3. A quantum mechanical description of the crossover from superexchange to TIH in $\text{G}^+(\text{T}-\text{A})_n \text{G}$ duplexes with increasing the bridge size. The solid lines with closed circles and triangles (—●— and —▲—) represent $|V_{\text{super}}|^2$ for the two duplexes marked on the figure. The dashed line with open squares (—□—) represents $|V_{\text{eff}}^{\text{TST}}|^2 = |V(\text{A}-\text{A})|^2 \exp(-\Delta/k_B T)/(n-1)$, with $\Delta = 0.22$ eV. The ‘critical’ size values, n_x , are marked by vertical arrows.

$$k_{\text{super}}(1) = \frac{2\pi}{\hbar} \left| \frac{V(\text{G}-\text{T})V(\text{T}-\text{G})}{\Delta(\text{G}-\text{T})} \right|^2 F(\Delta E). \quad (11)$$

The nuclear Franck–Condon factor, $F(\Delta E)$, Eqs. (5) and (6), depends on the energy gap ΔE between $\text{G}^+(\text{T})_n \text{GGG}$ and $\text{G}(\text{T})_n(\text{GGG})^+$. From a previous analysis [23] for G^+TGGG we take $\Delta E = -0.096$ eV, asserting that for charge shift ΔE is independent of n .

2.3. The ‘transition’

Considering parallel superexchange and TIH, we introduce a characteristic (T–A)_n bridge size, n_x , for the ‘transition’ between the two mechanisms. The superexchange dominates ($k_{\text{super}}(n) > k_{\text{TIH}}(n)$) at $n < n_x$, a crossover between the two mechanisms [49] will occur at $n = n_x$, where

$$k_{\text{super}}(n_x) = k_{\text{TIH}}(n_x) \quad (12)$$

and the TIH mechanism will dominate $k_{\text{super}}(n) < k_{\text{TIH}}(n)$ for $n > n_x$. Making use of Eqs. (3a),(4), (7),(8) and (12) we assert that the condition for the crossover is

$$\begin{aligned} |V_{\text{super}}|^2 F(\Delta E) \\ = |V(\text{A}-\text{A})|^2 [\exp(-\Delta/k_B T)/(n-1)] F(0). \end{aligned} \quad (13)$$

For symmetric hole transfer the nuclear Franck–Condon factors for k_{super} and k_{TIH} are approximately identical (both corresponding to $\Delta E = 0$), the crossover condition will be determined by the electronic couplings, being determined by the equation

$$\begin{aligned} n_x = 1 - \frac{\Delta}{k_B T \ln r} + \frac{\ln[|V(\text{A}-\text{A})|^2/|V_{\text{super}}(1)|^2]}{\ln r} \\ - \frac{\ln(n_x - 1)}{\ln r}. \end{aligned} \quad (14)$$

For hole trapping by GGG, a correction factor for the nuclear Franck–Condon factors with $F(0)/F(\Delta E_t)$, Eqs. (5) and (6), has to be incorporated.

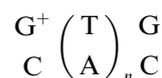
In Fig. 3 we present calculations for the superexchange–TIH crossover in $5'\text{-G}^+(\text{T})_n\text{-G-3'}$ and $5'\text{-G}^+(\text{A})_n\text{-G-3'}$ duplexes, where we portray the distance dependence of the electronic couplings for k_{TIH} and k_{super} and the superexchange TIH crossover (using the calculated pair matrix elements [58,59] and $\Delta = 0.20 \pm 0.05$ eV [49]). The contribution to TIH (in both cases via the (A)_n chain) is

Table 1
The ‘critical’ bridge size, n_x , in $G^+(T-A)_nG$ duplexes for the ‘transition’ from superexchange ($n < n_x$) to TIH ($n > n_x$)

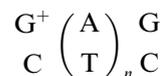
Duplex	Model and observable	Δ (eV)	n_x
$G \begin{pmatrix} T \\ C \end{pmatrix} \begin{matrix} G \\ A \end{matrix}_n C$	Kinetic–quantum mechanical model for rates (calculated)	0.22 0.17	4.0 3.3
$G \begin{pmatrix} A \\ C \end{pmatrix} \begin{matrix} G \\ T \end{matrix}_n C$	Kinetic–quantum mechanical model for rates (calculated)	0.22 0.17	4.4 3.7
$G \begin{pmatrix} T \\ C \end{pmatrix} \begin{matrix} G \\ A \end{matrix}_n C$	Kinetic–quantum mechanical model in kinetic limit for chemical yields (calculated)	0.22 0.17	(4.8) (3.9)
$G \begin{pmatrix} T \\ C \end{pmatrix} \begin{matrix} G \\ A \end{matrix}_n C$	Configurational relaxation accompanying hole injection for chemical yields (calculated)	0.17	3.1–3.6
$G \begin{pmatrix} T \\ C \end{pmatrix} \begin{matrix} G \\ A \end{matrix}_n C$	Experiment for chemical yields ^a	–	3–4

^a Ref. [48].

nearly invariant for the different duplexes, but some bridge specificity is manifested due to different contributions to $|V_{\text{super}}|^2$ (Fig. 3). The exponential distance (n) dependence for k_{super} and the algebraic distance dependence of k_{TIH} are exhibited. A superexchange–TIH crossover is manifested at $n_x \approx 3\text{--}4$ (with the n_x values marked in Fig. 3). n_x exhibits a bridge specificity, being lower by $\sim 15\%$ (Table 1) for the



duplex relative to the



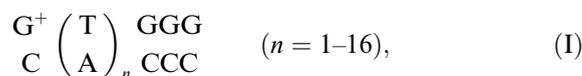
duplex. The dependence of n_x on the energy gap Δ (in the uncertainty range inferred from previous analyses [49]) is portrayed in Table 1, with n_x somewhat decreasing with lowering Δ in the appropriate energy region. This quantum mechanical–kinetic analysis for DNA infers that for ‘short’ $G^+(T-A)_nG$ or $(G)_\alpha^+(T-A)_n(G)_\beta$ ($\alpha, \beta = 1\text{--}3$) duplexes ($n < n_x$; $n_x = 3\text{--}4$) the superexchange mechanism dominates, with a nearly exponential distance dependence of the rates and chemical yields (see Section 3), while for long duplexes ($n > n_x > 4$) the TIH mechanism takes over, with a weak distance dependence of the rates and chemical yields (further considered in Section 3). The results of this analysis, which gives $n_x(\text{theory}) \sim 3\text{--}4$, are in reasonable agreement with the experimental results

for the superexchange–TIH crossover reported by Giese et al. ($n_x(\text{experiment}) \simeq 3\text{--}4$) [48]. As the available experimental information for long range (via superexchange) and very long range (via TIH) hole transport in DNA stems from chemical yield data, a more complete analysis of chemical yields will be desirable for the confrontation of our theoretical quantum mechanical–kinetic scheme with experimental reality.

3. A kinetic analysis of chemical yields

Giese and his colleagues [48] studied hole transfer in the duplexes ¹

¹ The experimental chemical yield data reported by Giese et al. [48] for their ‘new’ assay (assay II) at pH = 5 (Fig. 4) are considerably higher than their yield data (i.e., $R(1) = 30$, $R(2) = 3.2$, $R(3) = 0.44$, $R(4) = 0.03$) previously reported for their ‘old’ assay (assay I) at pH = 7 [36–38], where the hole injection process from the sugar cation is also different. The difference between assays I and II is attributed to the retardation of the reactions of G^+ and of $(GGG)^+$ with water (B. Giese, private communication). In our analysis we shall assume that the hole energetics (i.e., the energy difference between $G^+T \cdots T(GGG)$ and $GT \cdots T(GGG)^+$) and transfer kinetics is invariant in assay II with respect to assay I (analyzed in Refs. [21–23]), while the reaction rates of G^+ with water (k_r) and of $(GGG)^+$ with water (k_r) are different for the two assays. Indeed, the analysis in Section 2.1 shows that the value of $k_{\text{super}}(1)/k_r$ obtained herein for assay II is higher by a numerical factor of 3–10 than that previously obtained [21–23,36–38] for assay I, indicating the slowing down of the water reaction in assay II, as proposed by Giese et al. [48].



providing strong evidence for the ‘transition’ between superexchange (for $n = 3$) to TIH (for $n = 4-16$) and a weak bridge size (n) dependence for TIH. The relative chemical yield ratios $R(n)$ for a bridge length n , which are given by

$$R(n) = Y(\text{GGG terminal})/Y(\text{G proximal}),$$

exhibit the following features (Fig. 4) [48]:

(A) The superexchange region is characterized by an exponential n dependence, (Fig. 4).

(B) The ‘transition’ between superexchange and TIH is exhibited at $n_x \cong 3-4$ (Fig. 4) is in accord with our kinetic–quantum mechanical analysis, which predicts $n_x = 34$ (Section 2).

(C) The TIH process exhibits a very weak n dependence, (Fig. 4), with $R(n) = 2.5 \pm 0.5$ for $n = 5-16$.

We now proceed to explore the elementary rates and chemical yields in the kinetic scheme (Fig. 1) for the parallel superexchange–TIH mechanisms. This constitutes the extension of scheme (2) to incorporate the reaction with water.

3.1. Chemical yields for superexchange

The relative chemical yield for the superexchange mechanism is [23]

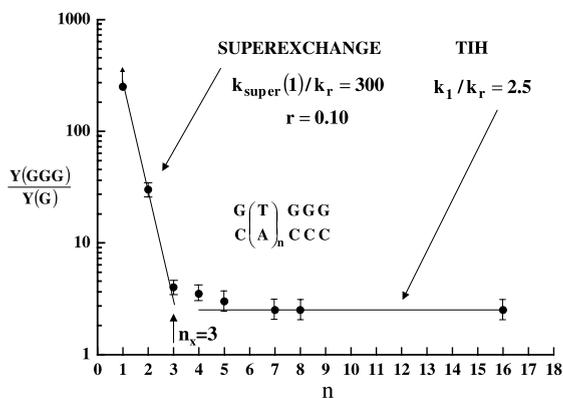


Fig. 4. The analysis of the experimental data (●) of Giese et al. [48] for the relative chemical yields in duplex (I) according to the modified kinetic–quantum mechanical model, Eqs. (23) and (24). The n_x value, Eq. (25), is marked by a vertical arrow.

$$R_{\text{super}}(n) = [k_{\text{super}}(n)/k_r][1 + (k_{\text{super}}(n)/k_{rt}) \times \exp(-\Delta E/k_B T)]^{-1}, \quad (15)$$

where $k_{\text{super}}(n)$, Eqs. (9)–(11), is the $\text{G}^+ \cdots \text{GGG}$ superexchange rate in duplex (I), ΔE is the $\text{G}^+ \cdots \text{GGG}$ energy gap and the rates k_r and k_{rt} for the water reactions of G^+ and $(\text{GGG})^+$, respectively, are defined in Eq. (A.1). The bridge length dependence of $R_{\text{super}}(n)$ is of the form $\alpha r^{n-1}/[1 + \gamma r^{n-1}]$, with $\alpha = k_{\text{super}}(1)/k_r$ and $\gamma = k_{\text{super}}(1) \exp(-\Delta E/k_B T)/k_{rt}$, exhibiting an exponential n dependence for large n , which may be flattened-off at low ($n = 1-2$) values due to the contribution of the γr^{n-1} term. From the experimental results of Giese et al. [48] we can infer that $k_{\text{super}}(1)/k_r \cong 300$ and $r = 0.1$ (Fig. 4). The value of r (or β), Eq. (10), for this experiment is close to the value $r = 0.07-0.1$ and $\beta = 0.7 \pm 0.1 \text{ \AA}^{-1}$ inferred from theoretical calculations [59] from the analysis of the yield data for Giese’s assay I [23,36–38] and from other experimental data by Lewis et al. [33–35,45] and by Zewail and co-workers [45]. Finally, the available experimental data do not show a deviation from exponential n dependence of $R_{\text{super}}(n)$ for $n = 1$. Accordingly, we assert on the basis of Eq. (15) that

$$(k_{\text{super}}(1)/k_{rt}) \exp(-\Delta E/k_B T) < 0.3.$$

As $\Delta E \cong 0.096 \text{ eV}$ we can assert that $k_{\text{super}}(1)/k_{rt} < 50$. From the estimates for $k_{\text{super}}(1)/k_r$ and for $k_{\text{super}}(1)/k_{rt}$, we infer that $k_{rt}/k_r > 5$. This estimated ratio of the reaction rates of $(\text{GGG})^+$ and of G^+ with water (for assay II) is (however not appreciably) higher than the ratio $k_{rt}/k_r = 1.8$ [47] and 3.6 [23] inferred from the previous analysis of the kinetic data for superexchange in Giese’s assay I [36–38].¹

3.2. Relative yields and rates for thermally induced hopping

The kinetic model for TIH (Fig. 1) is analyzed in Appendix A and results in the following compact expression for the relative chemical yield

$$R_{\text{TIH}} = \frac{(k_{rt}k_1k_t/k_r)}{k_{-t}k_{-1} + k_{rt}k_t + k_{rt}k_{-1} + (k_{rt}k_tk_{-1}/k)(n-1)}. \quad (16)$$

Making use of the detailed balance relations $k_1 = k_{-1} \exp(-\Delta E_1/k_B T)$ and $k_{-t} = k_t \exp(-\Delta G_t/k_B T)$, together with $\Delta E_t = \Delta E + \Delta E_1$, this expression can be recast in the alternative form

$$R_{\text{TIH}} = \frac{(1/k_r) \exp(-\Delta/k_B T)}{(1/k_{rt}) \exp(-\Delta E_t/k_B T) + [1/k_{-1} + 1/k_t + (1/k)(n-1)]}, \quad (16a)$$

where Δ is the G^+A-GA^+ energy gap, while ΔE_t is the trapping energy gap between A^+GGG and $A(GGG)^+$ (Fig. 1) and the elementary rates are defined in Fig. 1. Eq. (16) exhibits two limits:

(1) *The limit of equilibrium distribution.* When hole injection, trapping and hopping is extremely fast on the time scale of the water reaction

$$\frac{k_{rt}}{k_{-1}} + \frac{k_{rt}}{k_t} + \frac{k_{rt}}{k} (n-1) \ll \exp(-\Delta E_t/k_B T) \quad (17)$$

with some of the following rate ratios being very large, i.e.,

$$k_{-1}/k_{rt}, k_t/k_{rt}, k/k_{rt}(n-1) \gg \exp(\Delta E_t/k_B T) \quad (17a)$$

the equilibrium distribution is achieved. The relative chemical yields ratio in this case, R_{eq} , is given from Eq. (16) by

$$R_{\text{eq}} = (k_{rt}/k_r) \exp(\Delta E/k_B T), \quad (18)$$

where $\Delta E = \Delta E_t - \Delta$ is the energy gap between G^+ and $(GGG)^+$ (Fig. 1). The equilibrium distribution, Eq. (18), is independent of the bridge size n , as expected.

(2) *Kinetic limits.* When Eq. (17) is violated, Eq. (16a) holds. Of considerable interest is the kinetic limit when

$$k_{-1}/k_{rt}, k_t/k_{rt}, k(n-1)/k_{rt} < \exp(\Delta E_t/k_B T). \quad (19)$$

Eq. (16) then results in

$$R_{\text{TIH}} = \frac{(1/k_r) \exp(-\Delta/k_B T)}{1/k_{-1} + 1/k_t + 1/k(n-1)}. \quad (20)$$

The relative chemical yield in the kinetic limit, Eq. (20), manifests an algebraic bridge length (n) dependence of the form $R_{\text{TIH}} \propto [a + b(n-1)]^{-1}$, where the numerical constants are $a = (k_{-1})^{-1} +$

$(k_t)^{-1}$ and $b = k^{-1}$. A weak n dependence is expected to be manifested when $a \gg b(n-1)$, i.e.,

$$(n-1) \ll k/k_{-1} + k/k_t. \quad (20a)$$

It is instructive to relate the relative chemical yield in the kinetic limit, Eq. (20), to the hole residence time τ_1 in the initial state $G^+(A)_n GGG$. In Appendix A we show that in the absence of irreversible processes (e.g., the water reaction of G^+) this hole residence time is

$$1/\tau_1 \simeq \frac{\exp(-\Delta/k_B T)}{\in/k_{-1} + (n-1)/k}, \quad (21)$$

$$1/\tau_1 = \frac{1}{\in/k_1 + ((n-1)/k) \exp(\Delta/k_B T)}, \quad (21a)$$

where $\in = 1-2$ is a numerical constant depending on the relation between the rates k_{-1} and k_t (Appendix A). Considering for the moment extremely effective hole trapping ($1/k_t \rightarrow 0$), then the relative chemical yield in the kinetic limit assumes the form

$$R_{\text{TIH}} \cong (1/\tau_1)/k_r. \quad (22)$$

Eq. (22) provides a relation between relative chemical yields and residence lifetimes. Our result for R_{TIH} , Eqs. (21) and (22), can be expressed by the alternative relation, Eq. (21a), so that the hopping time $1/k$ (in the denominator) is multiplied by the reciprocal Boltzmann factor $\exp(\Delta_1/k_B T) \simeq 7 \times 10^3$. Segal et al. [60] (SNDWR) presented an important theoretical analysis for the initial state residence time τ^{SNDWR} in a symmetric donor-bridge-acceptor system, where the individual states are described in terms of one-level systems with dephasing. SNDWR obtained the following relation [60] for the residence time $1/\tau^{\text{SNDWR}} = 1/k_{\text{up}} + (1/k_{\text{diff}})n$. We can relate the rates of SNDWR to our rates in terms of $1/\tau^{\text{SNDWR}} \equiv 1/\tau_1$, $k_{\text{up}} \equiv k_1$ and $k_{\text{diff}} = k \exp(-E/k_B T)$. The present kinetic analysis concurs with the original model results of SNDWR [60].

We now proceed to the analysis of the TIH experimental data of Giese et al. [48] in duplex (II) ($n = 4-16$) in terms of the foregoing analysis, Eqs. (16)–(20). The first issue we address is whether these experimental results correspond to the limit

of equilibrium distribution or to the kinetic limit. The thermodynamic equilibrium limit is expected to be realized for $k/k_{rt} \gg \exp(\Delta E_i/k_B T)$ with $\Delta E_i \simeq 0.30$ eV (where $k = k_{-1}, k_t, k/(n-1)$). Making use of the relation $k_{rt}/k_r \simeq 5$ derived in Section 3.1, we require that $k/k_r \gg 8 \times 10^6$. From a quantum mechanical analysis of the elementary rates given below (Table 2), we conclude that the elementary rates k , together with $k_{\text{super}}(1)$, fall within the range of one-order-of-magnitude. Thus an order-of-magnitude estimate for the realization of the equilibrium distribution limit implies that $k_{\text{super}}(1)/k_r \gg 10^7$, while the analysis of the superexchange data (Section 2.1) results in $k_{\text{super}}(1)/k_r \simeq 300$. This 3–4 orders of magnitude discrepancy between the estimate of $k_{\text{super}}(1)/k_r$ and the onset of the thermodynamic limit, precludes the possibility of this equilibrium limit, whereupon the kinetic limit, Eq. (20), should be considered.

The analysis of the experimental data of Giese et al. [48] for the superexchange (for $n < 3$) and TIH (for $n = 4-16$) mechanisms leads us to a contradiction. We assert that our kinetic model, in conjunction with a quantum mechanical analysis of the elementary rates, infers that these experimental results [48] cannot be reconciled with the experimental TIH data. The fit of the experimental data [48] to Eq. (20) requires the fulfillment of two conditions.

(1) A weak n dependence of R . To account for the experimental observation (point (C) above), we have to utilize Eq. (20a), which implies that (for $n = 4-16$) $(n-1) \ll (k/k_t + k/k_{-1})$, implying that the rate determining steps should involve hole trapping processes.

(2) A proper description of the ratios of relevant elementary rates. The experimental TIH yield is $R = 2.5 \pm 0.5$ (for $n = 4-16$), whereupon, according to Eq. (20), $(k_r/k_{-1}) + (k_r/k_t) = 0.4 \exp(-\Delta/k_B T)$. These rate ratios are exponentially dependent on the energy gap Δ , i.e., for $\Delta = 0.22$ eV $(k_r/k_{-1}) + (k_r/k_t) \simeq 6 \times 10^{-5}$, while for a somewhat lower value of $\Delta = 0.17$ eV (which is still within the uncertainty range of Δ) $(k_r/k_{-1}) + (k_r/k_t) \simeq 4 \times 10^{-4}$.

These two conclusions for TIH have to be confronted with the results of the superexchange

Table 2
Rates for the elementary processes of TIH and superexchange in the duplex

Elementary process	Hole hopping in $(A)_n$ chain	'Thermal hole injection' from G^+ to $(A)_n$	'Hole trapping' from $(A)_n^+$ by G	'Hole trapping' from (A) by GGG	'Hole detrapping' from $(GGG)^+$ to $(A)_n$	Superexchange in G^+ TGGG
Rate constant	k	k_1	k_{-1}	k_t	k_{-t}	$k_{\text{super}}(1)$
Energy gap (eV)	0	$\Delta = 0.20 \pm 0.05$	$\Delta = 0.20 \pm 0.05$	$-\Delta E_t = 0.30 \pm 0.05$	$\Delta E_t = 0.30 \pm 0.05$	$-\Delta E = 0.096$
Relative Franck-Condon factors	1 ^a	1.9×10^{-3} ($\Delta = 0.22$)	12.5	44	1.8×10^{-4b}	5.4
$ V ^2$ (eV)	9×10^{-4}	1.4×10^{-2} ($\Delta = 0.17$) ^b	4×10^{-4}	1.6×10^{-5}	1.6×10^{-5}	4×10^{-4}
Relative rate	1 ^a	8.4×10^{-4} ($\Delta = 0.22$)	6.0	0.8	3.2×10^{-6}	2.5
Rate (s ⁻¹) ^c	5×10^7	4×10^4 ($\Delta = 0.22$)	3×10^8	4×10^7	1.6×10^2	1.2×10^8
		3×10^5 ($\Delta = 0.17$)				

^a Franck-Condon factors and rates for the hole hopping process (between adjacent A nucleobases) are normalized to unity.

^b Detailed balance relations are used, $k_1 = k_{-1} \exp(-\Delta/k_B T)$ and $k_{-1} = k_t \exp(-\Delta E_t/k_B T)$.

^c The absolute values of the elementary rates from the experimental rate for the hole hopping reaction [34] $G^+ AG \rightarrow GAG+$ ($k_{GAG} = 5 \times 10^7$ s⁻¹) for which $|V|^2 = 9 \times 10^{-4}$ (eV)², the energy gap = 0, the relative Franck-Condon factor is $F(0) = 1$ and the relative rate is 1.0.

analysis (Section 3.1), together with the (admittedly approximate) estimates of the six elementary rates $k_{\text{super}}(1)$, k_{-1} , k_1 , k_t , k_{-t} and k involved in the hole superexchange and TIH in duplex (I). Disregarding the explicit effects of static and dynamic configurational relaxations on the charge transfer dynamics, non-adiabatic electron transfer theory [19] can be applied. The superexchange rate $k_{\text{super}}(1)$ is estimated from Eqs. (7)–(12), with the electronic matrix elements taken from previous work [58,59] and the nuclear Franck–Condon factors taken from Eqs. (5) and (6). The hopping rates were estimated from Eqs. (4)–(6). The thermal excitation/deexcitation rates from/to $G(A)_n$ were taken as $k_1 = (2\pi/\hbar)|V(G/A)|^2 F(\Delta) \exp(-\Delta/k_B T)$ and $k_{-1} = k_1 \exp(\Delta/k_B T)$, where $V(G/A)$ is the interstrand G–A matrix element in duplex (I), while $F(\Delta)$ is given by Eqs. (5) and (6) with $\delta E = \Delta$. Finally, the trapping/detrapping rates from/to $(A)_n/(GGG)$ are given by $k_t = (2\pi/\hbar)|V(A \setminus G)|^2 F(\Delta E_t)$ and $k_{-t} = k_t \exp(-\Delta E_t/k_B T)$, where $V(A \setminus G)$ is the interstrand A–(GGG) matrix element in duplex (I), while the nuclear Franck–Condon factor is again given by Eqs. (5) and (6) with $\delta E = \Delta E_t$. The relative elementary rates estimated from the electron transfer theory (normalized to $k = 1$) are presented in Table 2. For the analysis of chemical yields, expressed in terms of rate ratios, only relative yields are required and will be used. We also present in Table 2 estimates of absolute values of the elementary rates inferred from the data of Lewis et al. [34] for hole hopping in G^+AG . From this analysis we infer that:

(1) The relevant (relative) elementary rates are $k_t \simeq 0.8$, $k \simeq 1$, $k_{-1} \simeq 6.0$ and $k_{\text{super}}(1) \simeq 2.5$, i.e., varying over a range of one order of magnitude.

(2) A failure to account for the weak n dependence of R by these elementary rates. In the experimental TIH range ($n = 4$ –16), we shall make use of Eq. (20a) and the data of Table 2, which result in $(k/k_t + k/k_{-1}) = 1.41$, while $(n - 1) = 3$ –15. Accordingly, $(n - 1) > (k/k_t + k/k_{-1})$ and Eq. (20a) is violated, resulting in a marked algebraic n dependence of $R \propto 1/(1.4 + (n - 1))$, in contrast with the experimental observation (point (C) above).

(3) Inconsistency between the ratios of elementary rates for superexchange and for TIH, which are inferred from the kinetic model and from the quantum mechanical electron transfer theory. The ratios of the rates $(k_r/k_{-1} + k_r/k_t) \simeq 6 \times 10^{-5}$ – 4×10^{-4} obtained above from the analysis of the experimental TIH data, together with the ratio for superexchange $k_{\text{super}}(1)/k_r$ (Section 3.1), imply that $k_{\text{super}}(1)/k_{-1} + k_{\text{super}}(1)/k_t \simeq 0.02$ – 0.012 . This estimate is lower by about two-orders of magnitude than the estimates based on the calculations of Table 2, which imply that $k_{\text{super}}(1)/k_{-1} + k_{\text{super}}(1)/k_t \simeq 3.5$. Accordingly, there is a marked discrepancy between the elementary rates inferred from the kinetic analysis and from the quantum mechanical model.

We thus conclude that the kinetic–quantum mechanical model does not account for two central quantitative features of the experimental data. First, the weak size (n) dependence of R and, second, the ratio of the elementary rates for superexchange and for TIH. The first issue reflects solely on the TIH mechanism. The second issue pertains to the description of both TIH and of superexchange. However, extensive previous analyses of superexchange mediated hopping and trapping via ‘short’ $(T-A)_n$ ($n \leq 4$) bridges [20–27] provide compelling support for the quantum mechanical model for superexchange, whereupon the second issue also presumably solely reflects on the failure of the description of the TIH.

4. Concluding remarks

So we arrived at a moment of truth, when a rather detailed analysis of chemical yield data for superexchange and TIH, although exhibiting a ‘reasonable’ estimate of the ‘critical’ bridge size n_x for the superexchange–TIH ‘transition’ (Table 1), reflects on the failure of the kinetic–quantum mechanical model. We note in passing that sometimes negative results are more interesting and stimulating than many-parameter fits of experimental data. One can and should attribute this failure of the kinetic–quantum mechanical model to the breakdown of the ‘hidden’ assumptions inherent in

our treatment of the TIH, which may include (among others): (i) The description of the hole hopping in the $(A)_n$ chain. (ii) The effects of dynamic disorder [61–63]. (iii) The effects of static disorder in the $(A)_n$ chain [19]. (iv) Configurational relaxation accompanying thermal hole injection from the G^+ to the $(A)_n$ chain.

Consider first the mechanism and dynamics of hole transport in the interconnected $(A)_n$ chain (point (i)). One can argue in this context that the very weak n dependence of R reflects an ultrafast hole transport in the $(A)_n$ chain due to a band-type motion, with a mean free path considerably exceeding the nearest-neighbor A–A spacing. Such a proposal, although being of considerable interest (and which cannot be excluded on the basis of the present yield data), will account for the weak n dependence of R , but cannot account for the inconsistency of the ratios of the rates of the other elementary reactions. A proper resolution of the conflict between experimental reality and the kinetic–quantum mechanical model for TIH requires the simultaneous resolution of the two issues.

Next, we address the possible effects of dynamic and static disorder in the $(A)_n$ chain. Regarding dynamic disorder (point (ii)) the effects of dynamic nuclear configurational fluctuations in DNA [61–63] on the rates of elementary processes of hole thermal injection, trapping/detrapping and hopping, may be of considerable importance. This may be due to the effects of dynamic fluctuations on the electronic couplings [62], energetics [63] and nuclear Franck–Condon factors. This interesting problem, which is intimately related to dynamic solvent effects [19] and to the role of fluctuations on the electronic coupling [62,64] in the theory of electron transfer, requires further exploration. Regarding the effects of static disorder in the $(A)_n$ chain, these may be due to aggregation and clustering of the adenine nucleobases [32], which are either inherently present in the ‘long’ chain or are induced by hole injection. Further structural information (from NMR data) will be of considerable interest regarding inherent structural disorder in these duplexes.

The possibility of ‘static’ configurational changes in the $(A)_n$ chain induced by hole injection to the $(A)_n$ chain in duplex (I) (mechanism (iv)) may

result in some interesting modifications of the TIH dynamics. It can be readily demonstrated that, provided that the hole backrecombination from $(A)_n^+$ to G is switched off, a proper description of TIH in duplex (I) can be readily provided. There is a distinct possibility that (fast) configurational relaxation accompanying thermally activated hole injection from G^+ to the $(A)_n$ chain may result in the gating (switching-off) of the $G(A)_n^+ \rightarrow G^+(A)_n$ backrecombination. Such a gating mechanism may be due to the drastic reduction of the G–A electronic coupling [58,59,62], or to hole trapping via proton transfer [65] in the A⁺–T Watson–Crick pair. As a phenomenological description of the gating mechanism we set $k_{-1} = 0$. Eq. (16) now results in the relation

$$R = k_1/k_r. \quad (23)$$

This simple analysis implies that R is independent of n and algebraic n dependence is not expected to set in even for very long bridges. Concurrently, the modified kinetic–quantum mechanical model is now applicable. Eq. (23), together with observation (C), results in $k_1/k_r \cong 2.5$ (for $n = 4$ –16) which, together with the superexchange data $k_{\text{super}}(1)/k_r \cong 300$ (Section 3.1), results in $k_1/k_{\text{super}}(1) < 8 \times 10^{-3}$. This result is in reasonable agreement with the ratio of the quantum mechanical elementary rates (Table 2), which give $k_1/k_{\text{super}}(1) \cong 3 \times 10^{-3}$ (for $\Delta = 0.17$ eV).

The experimental chemical yield data (Fig. 4) can be well accounted for in terms of the relations

$$R = \begin{cases} k_{\text{super}}(1)r^{n-1}/k_r, & n < n_x, \\ k_1/k_r, & n > n_x, \end{cases} \quad (24)$$

where $k_{\text{super}}(1)/k_r = 300$, $r = 0.1$ and $k_1/k_r = 2.5$. Eq. (24) constitutes the physical parameters determining the parallel superexchange/TIH mechanism, where the ‘transition’ bridge size is determined from the relation

$$n_x = 1 + [\ln(k_1/k_{\text{super}}(1))/\ln r], \quad (25)$$

where the ratio of the elementary rates $k_1/k_{\text{super}}(1) = 8 \times 10^{-3}$ from the kinetic analysis and $k_1/k_{\text{super}}(1) = 3 \times 10^{-3}$ from the quantum mechanical model, Eq. (25) and Table 2, results in $n_x = 3.1$ –3.5, in accord with the experimental value [48] $n_x = 3$ –4 (Table 1). We note in passing that the

The relative chemical yield is given by

$$R = \frac{Y_t}{Y_d} = \frac{k_{rt}}{k_r} \frac{k_1 k_t}{k_- k_- k_{-1} + k_t k_{rt} + k_{rt} k_{-1} + k_{rt} k_t k_{-1} (n-1)/k}. \quad (\text{A.7})$$

An equilibrium distribution is achieved when irreversible processes are relatively very small. The relative yield in such a situation is given by

$$R_{\text{eq}} = \frac{k_{rt}}{k_r} \frac{k_1 k_t}{k_- k_{-1}}, \quad (\text{A.8})$$

Eq. (A.7) can now be written as

$$R = \frac{R_{\text{eq}}}{1 + (k_{rt}/k_-)[1 + (k_t/k_{-1}) + k_t(n-1)/k]}. \quad (\text{A.9})$$

A.2. Effective rates

The residence time t_1 in the initial state, in the absence of irreversible processes at the initially oxidized nucleotide d , is evaluated as

$$\tau_1 = \int_0^\infty C_1(t) dt, \quad (\text{A.10})$$

where $C_1(t)$ is the time dependent concentration of the initial state ($C_1(0) = 1$). The dynamics of the system is governed by the kinetic equation

$$\dot{C}(t) = H' C(t). \quad (\text{A.11})$$

The rate constants matrix is given by

$$H' = \begin{pmatrix} -k_1 & k_{-1} & & & & & & & \\ k_1 & -(k+k_{-1}) & k & & & & & & \\ & k & -2k & k & & & & & \\ & & & \cdot & \cdot & \cdot & & & \\ & & & & k-2k & k & & & \\ & & & & k & -(k+k_t) & k_{-t} & & \\ & & & & & k_t & -(k_{-t}+k_{rt}) & & \end{pmatrix}. \quad (\text{A.12})$$

Here there is no water reaction at the initial site and therefore $k_r = 0$. The formal solution of the kinetic equation is

$$C(t) = \exp\{H't\}C(0); \quad C_1(0) = 1. \quad (\text{A.13})$$

So we get

$$\begin{aligned} \tau_1 &= \int_0^\infty C_1(t) dt = -\left[H^{-1}\right]_{1,1} \\ &= \frac{kk_t k_{rt} + (n-1)k_{-1}k_t k_{rt} + kk_{-1}k_{-t} + kk_{-1}k_{rt}}{kk_t k_1 k_{rt}}. \end{aligned} \quad (\text{A.14})$$

Several limiting cases are of interest:

1. A fast irreversible process ($k_{rt} \gg k_{-1}$):

$$\tau_1 \sim \frac{kk_t + (n-1)k_{-1}k_t + kk_{-1}}{kk_t k_1}. \quad (\text{A.15})$$

The effective rate constant is

$$k_{1,\text{eff}} = \frac{1}{\tau_1} = \frac{k_1}{k_{-1}} \frac{k}{(k/k_{-1}) + (k/k_t) + (n-1)}. \quad (\text{A.16})$$

2. In the symmetric case $k_t = k_{-1}$:

$$\tau_1 \sim \frac{(n-1)k_{-1} + 2k}{kk_1}. \quad (\text{A.17})$$

The effective rate constant is

$$k_{1,\text{eff}} = \frac{k_1}{k_{-1}} \frac{k}{2(k/k_{-1}) + (n-1)}. \quad (\text{A.18})$$

3. The asymmetric case $k_t \gg k_{-1}$

$$\tau_1 \sim \frac{(n-1)k_{-1} + k}{kk_1}, \quad (\text{A.19})$$

$$k_{1,\text{eff}} = \frac{k_1}{k_{-1}} \frac{k}{(k/k_{-1}) + (n-1)}. \quad (\text{A.20})$$

The final state accumulation time is given by

$$\begin{aligned} \tau_t &= \int_0^\infty (1 - C_{n+3}(t)) dt \\ &= \int_0^\infty \left(1 - k_{rt} \int_0^t C_{n+2}(s) ds\right) dt \\ &= \int_0^\infty \left(1 - k_{rt} \left[H'\right]^{-1} (\exp\{H't\} - 1)_{n+2,1}\right) dt. \end{aligned} \quad (\text{A.21})$$

Using the result $\left[H'\right]^{-1}_{n+2,1} = -1/k_{rt}$ we obtain

$$\tau_t = k_{rt} \int_0^\infty \left[\left[H'\right]^{-1} (\exp\{H't\})\right]_{n+2,1} dt = k_{rt} \left[\left[H'\right]^{-2}\right]_{n+2,1}. \quad (\text{A.22})$$

In the limit of large k_{rt} ($k_{rt} \gg k_{-t}$) one obtains

$$\tau_t = \frac{kk_t + kk_{-1} + (n-1)k_{-1}k_t}{kk_1k_t} + \frac{n}{k_t} + \frac{n(n-1)}{2k}. \quad (\text{A.23})$$

If also k_t is very large then

$$\tau_t = \frac{k + (n-1)k_{-1}}{kk_1} + \frac{n(n-1)}{2k}. \quad (\text{A.24})$$

References

- [1] A. Aviram, M.A. Ratner, Chem. Phys. Lett. 29 (1974) 277.
- [2] P. Sautet, C. Joachim, Phys. Rev. B 38 (1988) 12238.
- [3] V. Mujica, M. Kemp, A. Roitberg, M. Ratner, J. Chem. Phys. 104 (1996) 7296.
- [4] M. Magoga, C. Joachim, Phys. Rev. B 57 (1998) 1820.
- [5] R.A. English, S.G. Davison, Z.L. Miškovic, F.O. Goodman, J. Phys. Condens. Matter 10 (1998) 4423.
- [6] A. Onipko, Phys. Rev. B 59 (1999) 9995.
- [7] V. Mujica, A.E. Roitberg, M. Ratner, J. Chem. Phys. 112 (2000) 6834.
- [8] L.E. Hall, J.R. Reimers, N.S. Hush, K. Silverbrook, J. Chem. Phys. 112 (2000) 1510.
- [9] J. Jortner, M.A. Ratner (Eds.), Molecular Electronics, Blackwell, Oxford, 1998, p. 5-721.
- [10] C. Dekker, M.A. Ratner, Phys. Today 14 (8) (2001).
- [11] A. Marshall, J. Hodgson, Nat. Biotechnol. 16 (1998) 27.
- [12] S.O. Kelley, N.M. Jackson, M.G. Hill, J.K. Barton, Angew. Chem. Int. Ed. 38 (1999) 941.
- [13] C.A. Mirkin, R.L. Letsinger, R.C. Mucic, J.J. Stofhoff, Nature 382 (1996) 607.
- [14] A.P. Alivisatos, K.P. Johnsson, T.E. Wilson, C.J. Loveth, M.P. Bruchez, P.J. Schultz, Nature 382 (1996) 609.
- [15] E. Winfree, F. Lin, L.A. Wenzler, N.C. Seeman, Nature 394 (1998) 539.
- [16] E. Braun, Y. Eichen, U. Sivan, G. Ben-Joseph, Nature 391 (1998) 775.
- [17] H.W. Fink, C. Schönenberger, Nature 398 (1999) 407.
- [18] D. Porath, A. Bezryadin, S. de Vries, C. Dekker, Nature 403 (2000) 635.
- [19] M. Bixon, J. Jortner, Adv. Chem. Phys. 106 (1999) 35.
- [20] J. Jortner, M. Bixon, T. Langenbacher, M.E. Michel-Beyerle, Proc. Natl. Acad. Sci. USA 95 (1998) 12759.
- [21] M. Bixon, B. Giese, S. Wessely, T. Langenbacher, M.E. Michel-Beyerle, J. Jortner, Proc. Natl. Acad. Sci. USA 96 (1999) 11713.
- [22] M. Bixon, J. Jortner, J. Phys. Chem. B 104 (2000) 3906.
- [23] M. Bixon, J. Jortner, J. Phys. Chem. (in press).
- [24] V.A. Berlin, A.L. Burin, M. Ratner, J. Phys. Chem. A 104 (2000) 443.
- [25] F.C. Grozema, Y.A. Berlin, L.D.A. Siebbeles, J. Am. Chem. Soc. 122 (2000) 10903.
- [26] F.C. Grozema, Y.A. Berlin, L.D.A. Siebbeles, Int. J. Quantum Chem. 75 (1999) 1009.
- [27] Y.A. Berlin, A.L. Burin, M.A. Ratner, J. Am. Chem. Soc. 123 (2001) 260.
- [28] T. Holstein, Ann. Phys. N. Y. 325 (1959) 343.
- [29] G.B. Schuster, Acc. Chem. Res. 33 (2000) 253.
- [30] B. Giese, Acc. Chem. Res. 33 (2000) 631.
- [31] M.E. Nuñez, D.B. Hall, J.K. Barton, Chem. Biol. 6 (1999) 85,97.
- [32] T.T. Williams, D.T. Odon, J.K. Barton, J. Am. Chem. Soc. 122 (2000) 9048.
- [33] F.D. Lewis, X. Liu, J. Liu, S.E. Miller, R.T. Hayes, M.R. Wasielewski, Nature 406 (2000) 51.
- [34] F.D. Lewis, X. Liu, J. Liu, R.T. Hayes, M.R. Wasielewski, J. Am. Chem. Soc. 122 (2000) 12037.
- [35] F.D. Lewis, R.S. Kalgutkar, Y. Wu, X. Liu, J. Liu, R.T. Hayes, S.E. Miller, M.R. Wasielewski, J. Am. Chem. Soc. 122 (2000) 12346.
- [36] E. Megger, M.E. Michel-Beyerle, B. Giese, J. Am. Chem. Soc. 120 (1998) 12950.
- [37] B. Giese, S. Wessely, M. Spormann, U. Lindemann, E. Meggers, M.E. Michel-Beyerle, Angew. Chem. Int. Ed. 38 (1999) 996.
- [38] B. Giese, S. Wessely, Angew. Chem. Int. Ed. 39 (2000) 3490.
- [39] P.T. Henderson, D. Jones, G. Hampkian, Y. Kan, G.B. Schuster, Proc. Natl. Acad. Sci. USA 96 (1999) 8353.
- [40] L. Sani, G.B. Schuster, J. Am. Chem. Soc. 122 (2000) 11545.
- [41] S. Steenzen, S.V. Jovanovic, J. Am. Chem. Soc. 119 (1997) 617.
- [42] N.S. Hush, A.S. Cheung, Chem. Phys. Lett. 34 (1975) 11.
- [43] J. Saito, T. Nakamura, K. Nakatani, J. Am. Chem. Soc. 122 (2000) 3001.
- [44] A.A. Voityuk, J. Jortner, M. Bixon, N. Rösch, Chem. Phys. Lett. 324 (2000) 430.
- [45] C. Wan, T. Fiebig, S.O. Kelley, C.R. Treadway, J.K. Barton, A.H. Zewail, Proc. Natl. Acad. Sci. USA 96 (1999) 6014.
- [46] W.B. Davis, I. Naydenova, R. Haselsberger, A. Ogrodnik, B. Giese, M.E. Michel-Beyerle, Angew. Chem. Int. Ed. 39 (2000) 3649.
- [47] B. Giese, M. Spichty, Chem. Phys. Chem. 1 (2000) 195.
- [48] B. Giese, J. Amaudrut, A.K. Kohler, M. Spormann, S. Wessely, Nature 412 (2001) 318.
- [49] M. Bixon, J. Jortner, J. Am. Chem. Soc. (in press).
- [50] S.S. Isied, M.Y. Ogawa, J.F. Wishart, Chem. Phys. 92 (1992) 381.
- [51] C.C. Page, C.C. Moser, X. Chen, D.L. Dutton, Nature 402 (1999) 47.
- [52] M. Bixon, J. Jortner, M.E. Michel-Beyerle, Chem. Phys. 197 (1995) 389.
- [53] B. Hartwick, B. Bieser, T. Langenbacher, D. Muller, M. Richter, A. Ogrodnik, H. Scheer, M.E. Michel-Beyerle, Biophys. J. 72 (1998) 8.
- [54] I. Saito, T. Nakamura, K. Nakatani, Y. Yoshioka, K. Yamaguchi, H. Sugiyama, J. Am. Chem. Soc. 120 (1998) 12686.

- [55] K. Nakatani, C. Dohno, I. Saito, *J. Am. Chem. Soc.* 121 (1999) 10854.
- [56] H.A. Wegenknecht, S.R. Rajski, M. Pascully, E.D.A. Stemp, J.K. Barton, *J. Am. Chem. Soc.* 123 (2001) 4400.
- [57] K. Nakatani, C. Dohno, I. Saito, *J. Am. Chem. Soc.* 122 (2000) 5893.
- [58] A.A. Voityuk, N. Rösch, M. Bixon, J. Jortner, *J. Phys. Chem. B* 104 (2000) 9740.
- [59] A.A. Voityuk, J. Jortner, M. Bixon, N. Rösch, *J. Chem. Phys.* 114 (2001) 5614.
- [60] D. Segal, A. Nitzan, W.B. Davis, M.R. Wasielewski, M.A. Ratner, *J. Phys. Chem. B* 104 (2000) 3817.
- [61] T.E. Cheatham III, P.A. Kollman, *Ann. Rev. Phys. Chem.* 51 (2000) 435.
- [62] A.A. Voityuk, K. Siriwong, N. Rösch, *Phys. Chem. Chem. Phys.* (in press).
- [63] R.N. Barnett, C.L. Cleveland, A. Joy, U. Landman, G.B. Schuster, *Science* (in press).
- [64] Q. Xie, G. Archontis, S.S. Skourtis, *Chem. Phys. Lett.* 312 (1999) 237.
- [65] S.F. Steenken, *Free Rad. Res. Commun.* 16 (1992) 349.